ELSEVIER

Physics of the Earth and Planetary Interiors 100 (1997) 197–212

PHYSICS OF THE EARTH AND PLANETARY INTERIORS

A model for the layered upper mantle

Tibor Gasparik

Center for High Pressure Research, Department of Earth and Space Sciences, State University of New York at Stony Brook, Stony Brook, NY 11794, USA

Received 15 August 1995; accepted 21 May 1996

Abstract

Numerical modeling of mantle convection by Liu (1994, *Science*, 264: 1904–1907) favors a two-layer convection, if the results are reinterpreted for the correct phase relations in $(Mg,Fe)_2SiO_4$. The resulting chemical isolation of the upper and lower mantle suggests a highly differentiated and layered upper mantle to account for the discrepancy between the observed compositions of mantle xenoliths and the cosmic abundances of elements. It is shown that a layered upper mantle with a hidden reservoir can have a structure consistent with the observed seismic velocity profiles and an average bulk composition corresponding to the cosmic abundances. The evolution of the upper mantle and the origin of komatiites are discussed in the context of the proposed model. © 1997 Elsevier Science B.V.

1. Introduction

Major progress in our understanding of the Earth's interior has been made in the last decade, primarily owing to advances in seismology, experimental petrology, geochemistry and mineral physics. The evidence shows that the currently preferred models of a largely homogeneous Earth's mantle, such as pyrolite (Ringwood, 1962) or piclogite (Bass and Anderson, 1984), do not provide a satisfactory explanation of the new observations.

The present model for a layered upper mantle has been developed over the last 8 years in response to the new information obtained in phase equilibrium studies with a split-sphere anvil apparatus (USSA-2000) at the Stony Brook High Pressure Laboratory. The key information was the discovery of an alternative explanation for the 400 km discontinuity, corresponding to the transformation from pyroxene to garnet in compositions close to the enstatite–jadeite join (Gasparik, 1989). Until then, the transformation from $(Mg,Fe)_2SiO_4$ olivine to beta phase was the only explanation based on a phase transition. However, the concept of a refractory shell residing in the upper mantle (Gasparik, 1990a) was crucial in finding the way to incorporate the new information into a consistent model for the Earth's interior. Other important discoveries taking place at the same time have been essential for further developments and improvements of the model. This paper is an attempt to summarize the new evidence and propose a model for the mineralogy, chemistry, structure, and evolution of the upper mantle consistent with these observations.

2. Evidence for a layered mantle

Liu (1994) carried out numerical modeling of the effect of the transition from $(Mg,Fe)_2SiO_4$ spinel to

PII S0031-9201(96)03240-2

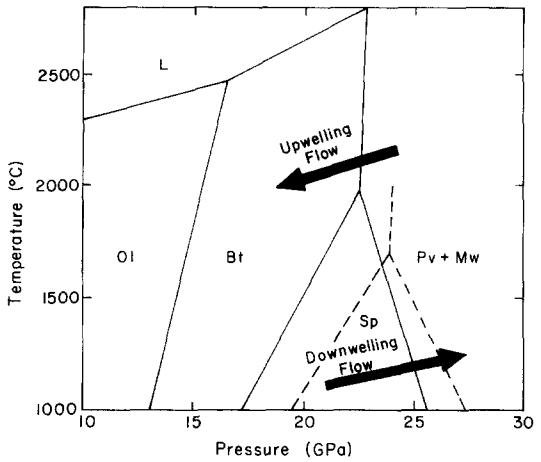

Fig. 1. Phase relations for Mg_2SiO_4 (continuous lines) and for lherzolite (dashed lines). Phases: Ol, olivine; Bt, beta phase; Sp, spinel; Pv, perovskite; Mw, magnesiowüstite; L, liquid. After Liu (1994).

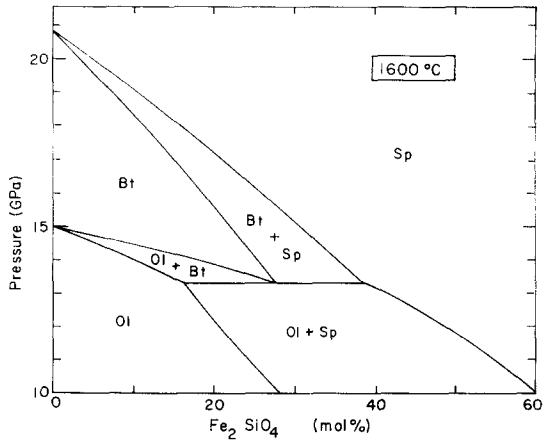

Fig. 2. Pressure–composition phase diagram for Mg_2SiO_4–Fe_2SiO_4 join at 1600°C. After Katsura and Ito (1989).

$(Mg,Fe)SiO_3$ perovskite and magnesiowüstite on mantle convection by considering two different cases. In the first case, the Clapeyron slope of the transition was negative at all relevant temperatures. Both downwelling and upwelling flows in the mantle were impeded by the negative slope, which resulted in a two-layer convection. In the second case, the slope of the transition changed from negative at lower temperatures to positive at higher temperatures. Consequently, whereas the downwelling flow was still impeded, hot plumes ascended across the positive boundary with ease. The resulting layering was much weaker and disappeared in a short time.

Liu (1994) favored the second case on the basis of his analysis of the phase relations reproduced in Fig. 1, where the phase boundaries for lherzolite were superimposed on the phase diagram for pure Mg_2SiO_4. However, even in chemically complex compositions, such as lherzolite, the three relevant polymorphs, olivine, beta phase and spinel, are still relatively simple binary solid solutions of Mg_2SiO_4 and Fe_2SiO_4. Phase relations in this binary system were experimentally determined several times, and are well established (Fig. 2). There is no doubt that the addition of iron to the system Mg_2SiO_4 expands the stability of spinel at the expense of beta phase to lower pressures. The phase relations used by Liu (1994) show the opposite, and thus are clearly incorrect.

The correct phase relations are shown in Fig. 3. The phase transition corresponding to the breakdown of spinel to perovskite and magnesiowüstite has a negative Clapeyron slope at all temperatures below the solidus, as considered by Liu (1994) in the first case. Thus, the flow of material across the 670 km discontinuity would be impeded in both directions, resulting in a two-layer convection (Knopoff, 1964; Anderson, 1979; Weinstein, 1992).

A major argument in favor of a layered mantle is the discrepancy between the olivine-rich composition of the primitive mantle derived from the compositions of mantle xenoliths (Ringwood, 1962; Jagoutz

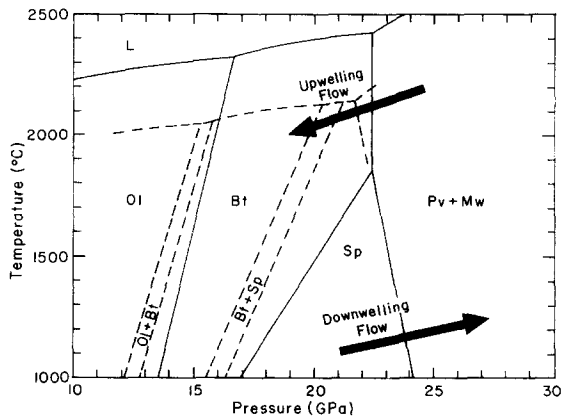

Fig. 3. Temperature–pressure phase relations for Mg_2SiO_4 (continuous lines) and $(Mg_{0.9}Fe_{0.1})_2SiO_4$ (dashed lines). Based on Katsura and Ito (1989), Ohtani et al. (1989), Gasparik (1990b) and Presnall and Walter (1993).

et al., 1979; Palme and Nickel, 1985) and the compositions of meteorites and the Sun, which have the Mg/Si ratio close to unity (e.g. Anders and Grevesse, 1989). Meteorites are considered to be representative of the material from which the Earth formed. Some meteorites did not undergo differentiation, others correspond to the material from differentiated, and subsequently disrupted, planetary bodies; these represent material from various layers in these bodies, and by analogy in the Earth. MacDonald and Knopoff (1958) were first to point out that a mantle corresponding in composition to chondritic meteorites would have to be composed mostly of pyroxene and garnet.

Mantle xenoliths typically originate at the depths less than 150–200 km. Because this observable part of the mantle is rich in olivine, a chondritic mantle has to be layered; a large-scale differentiation producing an olivine-rich upper layer requires the presence of a complementary silica-rich layer at greater depths. Liu (1979) suggested the possibility that the excess silica is concentrated in the lower mantle and the 670 km discontinuity is a chemical boundary between an olivine-rich upper mantle and a more silica-rich lower mantle. This could result from fractionation of $(Mg,Fe)SiO_3$ perovskite in a completely molten Earth (Kumazawa, 1981; Ohtani, 1985; Agee and Walker, 1988). However, Kato et al. (1988a,b)), Drake et al. (1993) and Gasparik and Drake (1995) showed conclusively that the perovskite fractionation is not consistent with the near-chondritic Ca/Al and Sc/Sm ratios observed in mantle xenoliths; a significant fractionation of $MgSiO_3$ perovskite from silicate melt during a magma ocean phase early in the Earth's history would cause these ratios to be distinctly nonchondritic.

Most recently, arguments based on the partitioning of siderophile elements between silicate melt and sulfur-bearing molten iron suggest that the extraction of iron from the observable mantle during core formation occurred at 28–30 GPa, thus at depths not exceeding greatly 670 km (Agee and Li, 1996; Righter et al., 1996). The experimentally determined melting curve of $(Mg,Fe)SiO_3$ perovskite shows a major increase in the melting temperatures with pressure at the low-pressure stability limit of perovskite (Zerr and Boehler, 1993; Sweeney and Heinz, 1995). The resulting deep cusp in the mantle solidus requires much higher magma ocean temperatures than necessary for the melting of the upper mantle to melt more than a minor portion of the lower mantle. If the melting curve of Sweeney and Heinz (1995) is correct, even a mantle-deep magma ocean would develop a perovskite septum at depths around 1000 km, effectively dividing the mantle into two regions, which could then crystallize and evolve separately. These considerations suggest that an early magma ocean responsible for the differentiation of the observable mantle was limited to depths not greatly exceeding 670 km.

A two-layered mantle is the minimum requirement when considering the geochemical evidence. For example, Hart (1988) used various isotopic data to make a case for at least four different reservoirs in the mantle. Arguments based on the noble gas systematics also require multiple reservoirs established very early in the Earth's history (Allègre, 1995; O'Nions and Tolstikhin, 1996). The evidence for a high degree of chemical isolation between the upper and lower mantle throughout most of the Earth's history thus appears robust.

3. Evidence for a hidden reservoir

The 400 km discontinuity has traditionally been explained by the phase transformation from $(Mg,Fe)_2SiO_4$ olivine to beta phase. Gasparik (1989) reported that the transformation from pyroxene to garnet occurring in compositions close to the enstatite–jadeite join at 130–135 kbar is univariant and thus could also produce a sharp discontinuity at the 400 km depth (Fig. 4). Continued advances in seismic techniques have since shown that the 400 km discontinuity is less than 2 km wide (Benz and Vidale, 1993). In contrast, the transformation from olivine to beta phase is divariant (Fig. 2) and would occur over a depth interval of 10–20 km (e.g. Katsura and Ito, 1989). Thus, the 400 km discontinuity cannot be caused by the transformation from olivine to beta phase, and the univariant transformation from pyroxene to garnet is now the most likely explanation.

If the mantle at 400 km depth has a composition close to the enstatite–jadeite join, it must be chemically stratified, because such a composition is very different from the compositions of mantle xenoliths.

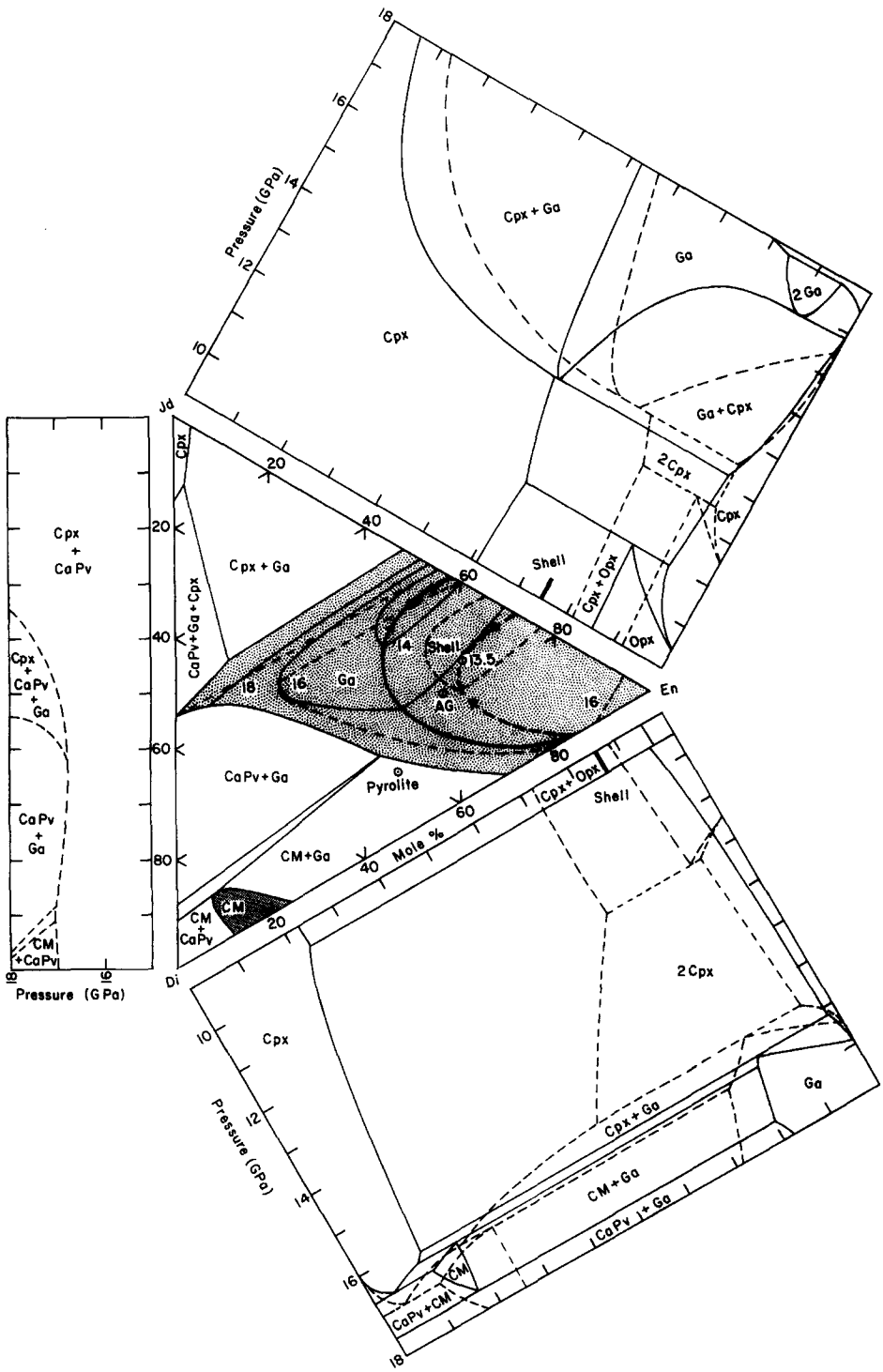
Pressure (GPa)
Cpx + Ga
Ga
2 Ga
Cpx
Ga + Cpx
2 Cpx
Cpx
Jd
Cpx + Ga
Shell
Cpx + Opx
Opx
En
Cpx + CaPv
Cpx + CaPv + Ga
CaPv + Ga
CaPv + Ga + Cpx
Ga
AG
CaPv + Ga
Pyrolite
CM + Ga
Mole %
Cpx + Opx
Shell
CM
CM + CaPv
Di
Pressure (GPa)
Cpx
2 Cpx
Ga
Cpx + Ga
CM + Ga
CaPv + Ga
CaPv + CM
CM

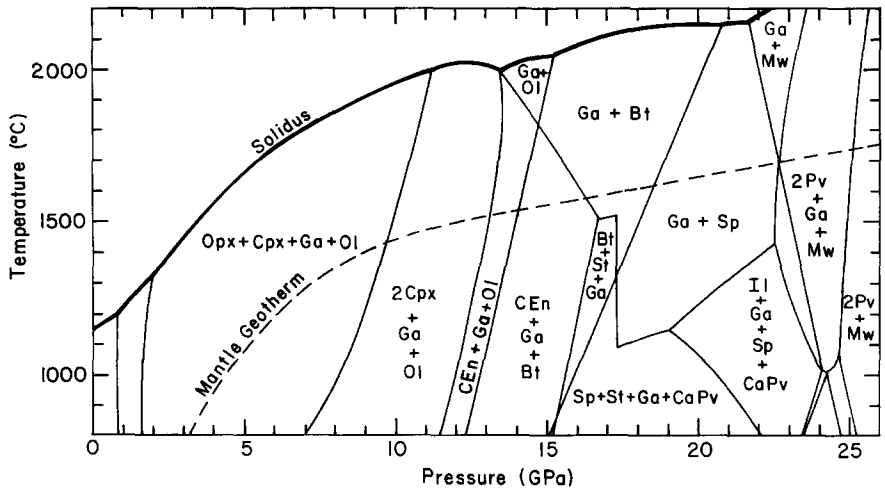

Fig. 5. Temperature–pressure phase relations for the proposed model of the Earth's upper mantle. CEn, Clinoenstatite; Il, ilmenite; Pv, perovskite; St, stishovite; other symbols as in Fig. 1 and Fig. 4. Based on data from Gasparik (1992, 1996a) and Herzberg and Gasparik (1991). Mantle geotherm is the model continental geotherm of Pollack and Chapman (1977) for the surface heat flow of 40 mW m^{-2}, with the adiabatic segment extrapolating to 1280°C at 1 bar (McKenzie and Bickle, 1988).

The relatively high sodium content suggests that the mantle at 400 km depth formed by crystallization of residual melts, presumably during the solidification of a magma ocean. The corresponding layer has to be refractory to remain preserved in the upper mantle throughout the Earth's history in spite of convection. Gasparik (1990a, 1992, 1993) proposed that this refractory shell is located between depths of 220 and 520 km, was completely dehydrated during its formation, and has remained unaffected by mantle processes owing to its extremely high melting temperatures exceeding 2000°C (Fig. 5). Another contributing, possibly even decisive, factor responsible for the refractory nature of the shell could be the high mechanical strength of majorite garnet predicted by Karato et al. (1995).

Additional evidence for a hidden reservoir is the observed depletion of the Archean mantle in incompatible elements, as is evident from the high Sm/Nd ratios of even the oldest Archean rocks (McCulloch and Compston, 1981; Basu et al., 1981; Hamilton et al., 1983; Shirey and Hanson, 1986; Galer and Goldstein, 1991). A complementary enriched reservoir formed by differentiation of the mantle prior to 3.8 Ga is required to balance this depletion. Because even the komatiite source regions were depleted, the enriched reservoir had to be located at depths greater than 200–300 km, which is the depth of origin of the oldest Barberton komatiites (Herzberg, 1992). It is proposed here that the enriched reservoir responsible for the depletion of the Archean mantle is in the shell.

4. Mantle convection

The presence of layering in the upper mantle is inconsistent with the whole mantle convection which would produce a homogeneous mantle. Such a mantle must be rich in olivine because that is the composition of the upper 200 km of the mantle accessible to observation through xenoliths. The idea of a ho-

Fig. 4. Phase relations in the enstatite–diopside–jadeite system at the mantle temperatures (T(°C) = 1280 + P(GPa)/0.055), shown by continuous lines, and at the solidus temperatures (T(°C) = 1880 + P(GPa)/0.055), shown by dashed lines. Shaded area is the stability field of garnet, with the isobars indicating the expansion of the garnet stability with pressure. Bold lines indicate the compositions of garnet coexisting with two pyroxenes; arrows point to a pressure minimum. Phases: Opx, orthopyroxene; Cpx, clinopyroxene; Ga,CM, garnet; CaPv, $CaSiO_3$ perovskite. Calculated from the data of Gasparik (1989, 1992, 1996a,b).

mogeneous mantle received widespread support with the discovery of plate tectonics, which revealed a highly dynamic nature of the Earth's surface consistent with a vigorously convecting interior.

A two-layered mantle is expected to have independent convection regimes in the upper and lower mantle, separated by the mostly impermeable 670 km discontinuity. A major argument against this view is the evidence from tomography suggesting that some slabs penetrate into the lower mantle. As will be discussed later, this could either be a very recent development in the evolution of mantle dynamics, or may not occur in some cases. The evidence is subject to interpretation of the tomographic images, in which the lower velocities are traditionally associated with higher temperatures (e.g. Anderson et al., 1992). However, the presence of an interstitial volatile-bearing melt would have the same effect. In extreme cases, the observed contrast in seismic velocities is so great that the corresponding temperature contrast would be unrealistic, and the presence of melt is the only plausible explanation (Zielhuis and Nolet, 1994). Some of the seismically slowest regions on the global scale are situated above the subducting slabs, and most likely reflect partial melting caused by the volatiles released from the slabs (Revenaugh and Sipkin, 1994; Nolet et al., 1994). As a slab warms up to sufficiently high temperatures during subduction, partial melting of the slab is likely to occur in the transition zone (400–670 km), owing to the presence of volatiles (Gasparik, 1993). As the degree of partial melting of a slab increases with increasing temperature, the effect of the melt on the seismic velocities could more than compensate for the low temperature of the slab. At the same time, the underlying mantle is cooled by the slab, and could potentially attain even higher velocities than the adjacent slab. Such velocity inversion would obscure the continuation of the slab in the transition zone and can result in a false image of the slab descending into the lower mantle.

Another argument against a two-layered mantle is the large size of the oceanic plates, which is more consistent with whole mantle convection; convection cells limited to the upper mantle would have to be extremely flat. But even the two-layered convection model does not allow for layering within the upper mantle. Hence, the potential presence of such layering requires a major revision of our views on mantle convection.

Gasparik (1993) proposed that a significant transport by convection may only occur in the presence of an interstitial melt. This study concluded that the expected mantle temperatures are higher than the temperatures of the volatile solidus; hence, in the presence of volatiles, the mantle should be partially molten. Van den Berg et al. (1993) pointed out that the experimentally determined high melting temperatures of $(Mg,Fe)SiO_3$ perovskite (Zerr and Boehler, 1993) would prohibit convection in the lower mantle unless the melting temperatures are decreased by volatiles. Any estimate of the rheological properties of the Earth, for example from a postglacial uplift, would reflect the properties of a partially molten Earth, and cannot be used in support of the solid-state convection. This view allows a convection regime in which any volatile-free, completely solid region potentially present in the mantle is mostly excluded from convection. In this case, the rheological properties of the deep mantle would be analogous to the properties of the Earth's crust, where the sharp contrast between the rheology of the solid and the partially molten rocks is evident.

The purpose of this line of reasoning is to suggest an explanation for the inferred relative immobility of the transition zone (e.g. Ringwood, 1994) and for the preservation of deep roots under some continents (MacDonald, 1963; Jordan, 1975). It is proposed that the region between depths of 220 and 520 km, corresponding to the refractory shell, is excluded from convection because it was completely dehydrated during its formation from the magma ocean. Thus, whereas convection can take place in the whole lower mantle owing to the ubiquitous presence of volatiles, convection in the upper mantle is limited to the volatile-bearing regions, which include the oceanic lithosphere, asthenosphere, transition zone between 520 and 670 km depth, and the narrow conduits associated with the spreading centers, subduction zones and hotspots.

The presence of volatiles is essential for the recycling of the subducted oceanic lithosphere. Tomographic images of subduction zones indicate that slabs maintain their rigidity and integrity in the upper mantle, encounter resistance at the 670 km discontinuity, and could stall there and be overrun by

the upper mantle. Ultimately, the slabs seem to soften; they deform, thicken and bend, and are inserted in the transition zone between 520 and 670 km depth (Van der Hilst et al., 1991; Fukao et al., 1992). This behavior is consistent with an incipient melting expected in the presence of volatiles during the process of thermal equilibration of the slab with the surrounding mantle, and is similar to the behavior implied by Ringwood and Irifune (1988).

A slab anchored at the 670 km discontinuity could lose support owing to the incipient melting caused by volatiles. This could result in a sudden movement of the slab with respect to the surrounding mantle, potentially triggering deep-focus earthquakes (Gasparik, 1993). Such a mechanism is consistent with the Bolivian earthquake of 1994, which was apparently caused by a sudden movement along a preexisting hydrated fault and was triggered by the lubricating effect of the released volatiles (Silver et al., 1995).

In the presence of volatiles, the whole slabs residing in the transition zone could ultimately turn into crystal mush on further heating. This is supported by several recent viscosity models, which predict a low-viscosity layer in the transition zone (Ricard et al., 1989; Forte et al., 1991; King and Masters, 1992). The slabs are then completely recycled by upwelling under the spreading centers. At the speeds of upwelling in meters per year, the conduits feeding the spreading centers need to be only a kilometer wide to allow for the complete recycling of the oceanic lithosphere. Such narrow conduits could not be detected by seismic methods.

The distribution of the conduits in the shell controls the position of plate boundaries and hotspots on the surface of the Earth. A minor mismatch between the plate boundaries and the system of conduits in the shell can be compensated by flow in the asthenosphere, along which the two systems of plates are decoupled. A major mismatch results in the secession of spreading, displacement of hotspots, and breakup of continents.

5. Chemical composition and phase relations

The current mantle models based on the compositions of mantle xenoliths, such as pyrolite (Ringwood, 1962), are not likely to give the correct estimate for the composition of a layered mantle, especially in the presence of a hidden reservoir. A more reliable estimate should be based on the cosmic abundances of elements.

If the transition zone is a graveyard for the subducted oceanic lithosphere, it can be assumed that the upper mantle to the depth of 150 km and the transition zone between 520 and 670 km depth, which together comprise 45% of the upper mantle, have the pyrolite composition. The remaining 55% is considered to correspond to the remains of the refractory shell. The composition of the shell was calculated by subtracting the pyrolite portion of the upper mantle from the cosmic abundances of Anders and Grevesse (1989).

The result is given in Table 1. An average shell should be composed of 37% of modal olivine and 63% of pyroxene. Because the sodium and aluminum contents of the shell are the same, the pyroxene composition can be fully expressed in terms of three components, enstatite, diopside and jadeite, if the relatively small amount of iron is included with magnesium. Phase relations in this ternary system were determined (Gasparik, 1989, 1992, 1996a,b),

Table 1
Estimates of the chemical composition of the Earth's upper mantle (atoms per 1000 Si), corresponding modal contents of olivine and pyroxene, and the pyroxene components (mole per cent)

Element	Anders and Grevesse (1989)	Pyrolite	Shell
Si (Si + Ti)	1000	1000	1000
Al (Al + Cr)	98	107	91
Mg (Mg + Mn)	1082	1255	940
Fe	126	146	110
Ca	61	73	51
Na (Na + K)	60	21	91
Olivine	48	60	37
Pyroxene	52	40	63
Enstatite ($Mg_2Si_2O_6$)	49.5	31.7	60.4
Diopside ($CaMgSi_2O_6$)	19.4	27.7	14.2
Jadeite ($NaAlSi_2O_6$)	19.0	8.0	25.4
Pyrope ($Mg_{1.5}AlSi_{1.5}O_6$)	12.1	32.6	0

The Fe/(Fe + Mg) ratio in the cosmic abundances of Anders and Grevesse (1989) is the same as in pyrolite from Table 8-1 of Anderson (1989); Fe is included with Mg in the pyroxene components.

and an updated phase diagram is shown in Fig. 4. The diagram shows the phase relations at the temperatures corresponding to the adiabatic portion of the mantle geotherm, and thus relevant to the present mantle, and at the solidus temperatures relevant to the formation of the shell by solidification of a magma ocean.

The calculated composition of the shell is identical to the composition of the first garnet forming in the ternary system from two pyroxenes at the solidus temperatures and the pressure corresponding to 400 km depth. This would be an unlikely coincidence unless the average composition of the shell is controlled by the crystallization of garnet.

At the present mantle temperatures and pressures less than 13 GPa, the shell composition produces an assemblage of two pyroxenes and olivine. At the pressure corresponding to 400 km depth, the jadeitic pyroxene transforms to garnet. This transformation is univariant, and thus can produce a sharp discontinuity consistent with the seismic observations of the 400 km discontinuity. An important requirement for a sharp discontinuity in this case is the absence of the pyrope–grossular–almandine component in garnet, which would smear the transformation to lower pressures (Gasparik, 1989). The calculated shell composition satisfies this requirement. At higher pressures, the enstatite-rich pyroxene dissolves in the garnet. This process is completed at 490 km depth, where the pyroxene portion of the shell transforms fully to garnet.

A simplified temperature–pressure phase diagram for the proposed upper mantle is shown in Fig. 5. This diagram accounts for the effect of all major elements on the phase relations, and is based on an updated diagram for the system $CaO–MgO–Al_2O_3–SiO_2$ (Gasparik, 1990b, 1996a; Herzberg and Gasparik, 1991), which was corrected for the effects of sodium (Gasparik, 1992) and iron (Ohtani et al., 1991). With increasing pressure along the mantle geotherm, the phase boundaries shown correspond to the transformation of orthopyroxene to the high-pressure polymorph of enstatite-rich clinopyroxene, the transformation of jadeitic clinopyroxene to garnet responsible for the 400 km discontinuity, the transformation of olivine to beta phase occurring at around 420 km depth, the high-pressure stability limit of enstatite-rich clinopyroxene at 490 km, the transformation of beta phase to spinel in a limited depth range around 560 km, the breakdown of spinel to perovskite and magnesiowüstite responsible for the 670 km discontinuity, and the high-pressure stability limit of garnet at 750 km. A chemical boundary at 520 km depth between the shell and the subducted slabs is reflected primarily in the garnet composition by an increase in the pyrope content of garnet from zero in the shell to about 30 mol % in pyrolite. This causes a major expansion in the stability of the two-phase assemblage of garnet and spinel to lower temperatures.

6. Mineral composition of the upper mantle

The corresponding mineral composition of the upper mantle can be calculated using the bulk compositions given in Table 1 and the phase relations from Fig. 4 and Fig. 5. The result is shown in Fig. 6 and Fig. 7. Fig. 6 summarizes the upper-mantle mineralogy under the assumption that the two chemically distinct units, the oceanic lithosphere and the shell, are homogeneous. A transition region is included between the depths of 100 and 200 km to account for the likely mixing of the two units in the asthenosphere. In this region, the olivine content decreases from 60 to 37%, the pyropic garnet is eliminated, and the clinopyroxene increases, changing in composition from diopsidic to jadeitic. The subducted oceanic lithosphere consists of only two phases, garnet and an $(Mg,Fe)_2SiO_4$ polymorph (beta

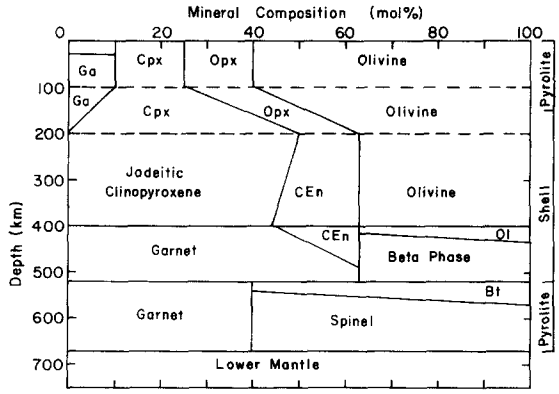

Fig. 6. Mineral composition of an upper mantle with chemically homogeneous layers of pyrolite and shell.

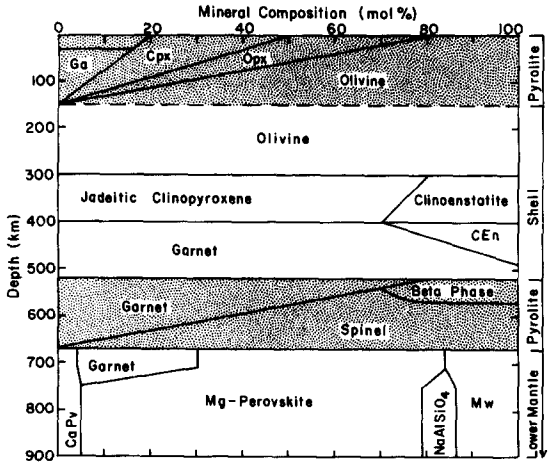

Fig. 7. Mineral composition of a layered upper mantle. Shaded layers correspond to oceanic lithosphere.

phase or spinel). At 400 km depth, jadeitic clinopyroxene transforms to garnet, and at 415–435 km, olivine transforms to beta phase.

A major problem with this 'homogeneous' model is that, in addition to a sharp discontinuity at 400 km depth, there would be another, more gradual discontinuity at slightly greater depths, caused by the transformation from olivine to beta phase. Moreover, this model cannot explain the presence of the high-velocity gradients in the slab portion of the transition zone (e.g. Bass and Anderson, 1984; Rigden et al., 1994). These discrepancies can be eliminated by adopting a layered model.

In the layered model (Fig. 7), the layering reflects the crystallization of liquidus phases in a magma ocean. The accumulation of olivine at shallow depths by olivine flotation is expected to produce an olivine septum at 150–300 km depth (Stolper et al., 1981; Agee and Walker, 1988, 1993; Ohtani et al., 1993, 1995). The crystallization of garnet at greater depths forms a garnet layer in the transition zone (Anderson, 1982). The shell composition crystallizes primarily as pyroxene between 300 and 400 km depth. The 400 km discontinuity is the boundary between the pyroxene and the garnet layer, and a chemical

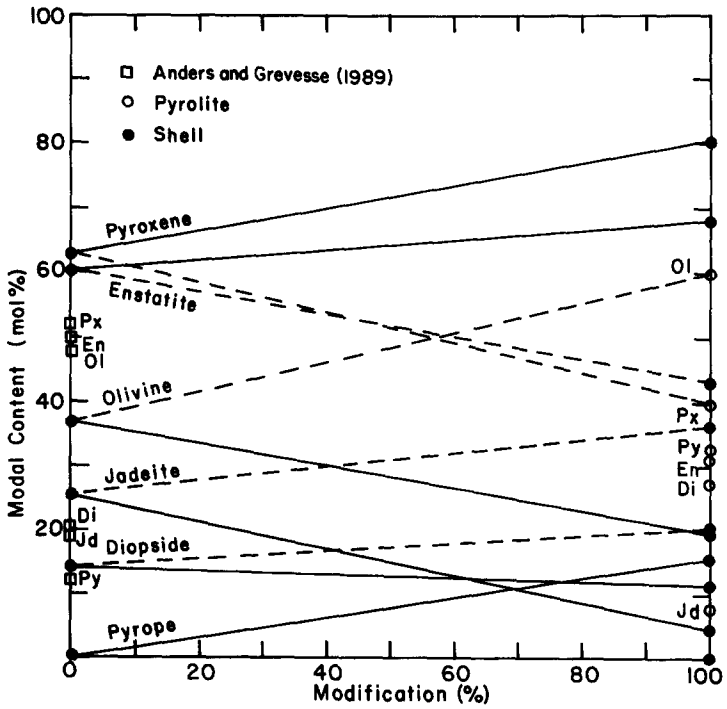

Fig. 8. Variations in the modal contents of olivine, pyroxene, and pyroxene components resulting from two different modifications of the proposed model (see text).

boundary between the shell and the subducted slabs is at 520 km depth. Inherent compositional variations in the slabs residing between 520 and 670 km depth are expected to cause a gradual change in the mineral composition with depth from garnet to spinel, responsible for the observed high-velocity gradients in this region (Gasparik, 1993). The 670 km discontinuity is both a phase and a compositional boundary, and the composition of the lower mantle is cosmic.

Finally, two possible modifications of this model are considered (Fig. 8). The first modification, indicated in Fig. 8 by continuous lines, assumes that the Earth does not have the high sodium content implied by the cosmic abundances of Anders and Grevesse (1989), perhaps because sodium, being a volatile element, was lost during the giant impact which produced the Moon and was probably responsible for the formation of the magma ocean on Earth (Hartmann and Davis, 1975; Wetherill, 1976; Cameron and Ward, 1976; Cameron and Benz, 1991). The observed low sodium content of the Moon supports this assumption. The chosen boundary case for the composition of the upper mantle has the sodium content of pyrolite. This would result in a major decrease in the jadeite content, thus eliminating the possibility that the 400 km discontinuity is caused by the transformation from pyroxene to garnet. However, this would also result in a major decrease in the olivine content from 37 to 20%, which is insufficient to explain the 400 km discontinuity by the transformation from olivine to beta phase. In this case, the discontinuity would be much smaller, more gradual, and present at greater depths than observed.

The second modification, shown in Fig. 8 by dashed lines, assumes that the fractionation in a magma ocean led to a higher average iron content in the shell than in pyrolite, because the residual melt was likely to be enriched in iron. This would increase the olivine content of the shell. The chosen boundary case for the composition of the upper mantle has the olivine content of pyrolite. The resulting pyroxene content is lower, thus its jadeite content is higher, which will be reflected in a higher proportion of the jadeitic clinopyroxene with respect to the enstatite-rich clinopyroxene. Because it is the transformation of the jadeitic clinopyroxene which causes the 400 km discontinuity, this modification of the model is consistent with the observations.

7. Evolution of the upper mantle

The simplest explanation for the inferred layering of the upper mantle is the well-documented change in the liquidus phase with depth from olivine to garnet and its effect, taking place during the solidification of a magma ocean, on the mineralogy, chemistry and structure of the upper mantle. However, simple fractionation of these liquidus phases is inconsistent with some observations.

It is now accepted that olivine becomes buoyant in ultramafic melts at a depth around 300 km (Rigden et al., 1984; Agee and Walker, 1988; Miller et al., 1991). It is not clear that this will happen in the more silica- and sodium-rich residual melts formed by partial crystallization of a chondritic mantle. The effect of garnet fractionation on the near-chondritic Ca/Al ratio of the observable upper mantle allows 10–30% of garnet fractionation (Herzberg and Gasparik, 1991). However, this amount of garnet fractionation would deplete the observable mantle in heavy rare earth elements, in contrary to what is observed. In addition, arguments were made that vigorous convection in a magma ocean could prevent fractionation (Tonks and Melosh, 1990; Solomatov and Stevenson, 1993).

The only kind of fractionation that does not seem to cause problems is the fractionation of olivine. Accumulation of olivine at shallow depths is necessary to account for the elevated Mg/Si ratio of the observable mantle. Such fractionation could leave the residual melt sufficiently rich in sodium and silicon to produce a garnet-rich layer in the transition zone even without garnet fractionation.

The proposed evolution of the upper mantle is shown in Fig. 9, starting with the crystallization of a magma ocean resulting from the giant Moon-forming impact. Owing to the oblique nature of the impact, only about 30% of the mantle melts. The magma engulfs the remaining unmelted portion of the Earth, producing a magma ocean of a uniform depth, approximately corresponding to the upper mantle (Stevenson, 1987; Tonks and Melosh, 1993). Crystallization starts when the temperature drops below the liquidus, thus precipitating liquidus phases (Fig. 9(a)). Vigorous convection may prevent the fractionation of olivine or garnet. Thin crust composed mainly of olivine forms at the surface, sinks and

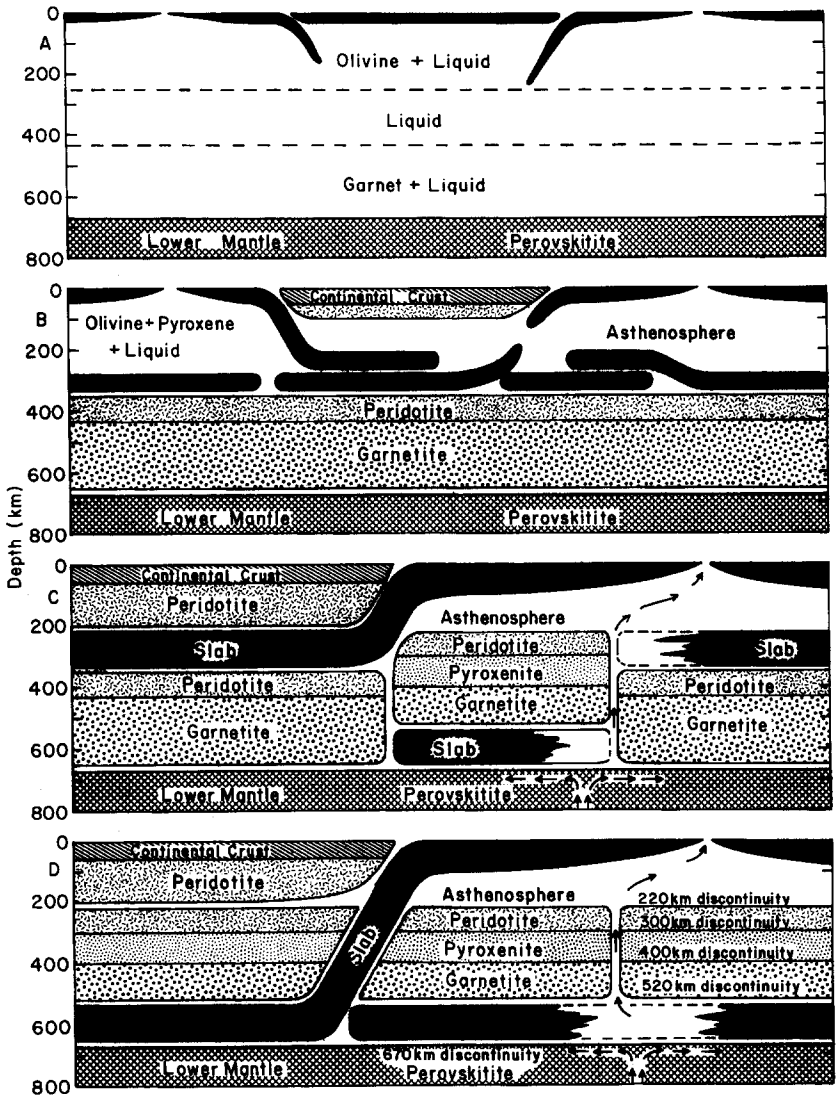

Fig. 9. Evolution of the Earth's upper mantle (see text).

dissolves before reaching the bottom of the magma ocean. With further cooling and corresponding increase in viscosity of the magma ocean, the crust becomes thicker and sinks and dissolves more slowly. If the rate of formation of the crust is faster than dissolution, the olivine-rich crust will accumulate in the upper 200 km of the magma ocean before sinking to deeper levels and dissolving. Partial segregation of the residual melt may occur as the crust accumulates preferentially at the centers of convecting cells (see also Ohtani, 1985; Agee and Walker, 1988; Tonks and Melosh, 1990; Abe, 1993; Morse, 1993).

The residual olivine-depleted melt crystallizes in the transition zone, producing a garnet-rich layer (Fig. 9(b)). Because the dP/dT slope of the solidus at the corresponding pressures is close to adiabatic (Fig. 5), the whole garnet layer may solidify at the same time, thus minimizing the possibility of garnet

fractionation. The crust starts accumulating at the top of the highly viscous and mostly solid garnet layer. This cools the top of the garnet layer and produces a barrier which prevents further mixing between the two regions. The garnet layer completely solidifies, forming a refractory shell. Continental crust segregates subsequently from the depleted olivine-rich asthenosphere.

Fig. 9(c) shows the upper mantle in the Archean. The garnet shell breaks into segments, perhaps owing to the contraction on further cooling and to the slowdown in the Earth's rotation (Dicke, 1969). Subduction is predominantly shallow (McCulloch, 1993; Rapp and Shimizu, 1996). The oceanic crust is recycled by partial melting in hot slabs. However, colder slabs dehydrate before melting, because the interval between the dehydration and the melting temperatures at the corresponding pressures is several hundred degrees Celsius, and the H_2O fluid escapes. As the presence of H_2O in the slabs is deemed essential for recycling, such dehydrated slabs cannot be recycled and accumulate in the asthenosphere. Thus, colder regions of the asthenosphere, particularly under continents, are filled with nonrecyclable dehydrated slabs, forming the deep roots of some continents. On rare occasions, the oldest and thickest slabs penetrate through the shell and are inserted between the shell and the lower mantle. This raises the overlying segment of the shell, and the garnet from the top portion of the segment transforms to pyroxene.

The post-Archean upper mantle is shown in Fig. 9(d). Most of the oceanic plates are sufficiently thick to be able to subduct to the top of the lower mantle, and this type of subduction has become dominant. The slabs are now cold enough to carry hydrous phases to the transition zone. Because the interval between the dehydration and the melting temperatures in the transition zone is narrow or absent, the slabs are again fully recycled by partial melting (Gasparik, 1993). The garnet shell has been displaced to shallower levels world-wide, as is evident from the global occurrence of the 400 km discontinuity. The evidence from tomography suggests that, at present, some of the oldest slabs seem to be able to penetrate into the lower mantle. It is proposed that this style of subduction has developed only recently and its contribution to the mixing between the upper and lower mantle has been minimal, in agreement with the limited mixing suggested by the noble gas systematics (O'Nions and Tolstikhin, 1996).

8. The origin of komatiites

Komatiites have received increased attention in recent years, since it was understood that komatiitic melts originated at much higher pressures and temperatures than the more common basaltic melts (Bickle et al., 1977). Numerous experimental studies have shown that the komatiitic melts have the compositions of the partial melts forming on the anhydrous solidus of common mantle compositions (e.g. Herzberg et al., 1990; Wei et al., 1990). Thus, the compositions of komatiites are controlled by phase relations rather than the bulk composition of the source region (Arndt, 1986). This makes it possible to estimate the depth of origin of the komatiitic melts and the temperature of the source region from experimental studies of melting relations.

Herzberg (1992) discussed the experimental evidence indicating that all komatiitic melts formed at pressures lower than 10 GPa, and that the age and depth are correlated; older komatiites originated at greater depths (see also Takahashi (1990)). For example, the 3.5 Ga Barberton komatiites originated at 240–300 km depth, whereas the Mesozoic Gorgona komatiites originated at 120 km depth. Herzberg (1992) estimated that the Barberton komatiites required a source region which was 500°C hotter than the present mantle. It is proposed here that the komatiitic volcanism occurred as the direct consequence of the thermal structure of the upper mantle formed by the solidification of the magma ocean.

The refractory shell produced during the solidification of the magma ocean could cool only by conduction, and thus cooled much slower than the convecting asthenosphere located closer to the Earth's surface. Knopoff (1964) calculated that in a nonconvective Earth, the surface would receive heat only from the uppermost 400–600 km in the lifetime of the Earth. Hence, the cooling of the 300 km thick shell could have occurred throughout a major span of the Earth's history, comparable with the age span of komatiites. At the time of solidification, the shell was sufficiently hot to generate the most magne-

sium-rich komatiitic melts required, for example, for the Barberton-type komatiites, and its slow cooling throughout the Earth's history could have produced the whole range of temperatures necessary for the origin of the younger komatiites. The absence of komatiitic volcanism after the Mesozoic indicates that the shell has reached thermal equilibrium with the surrounding mantle. This is supported by the observed correlation between the age of komatiites and the depth of origin or the temperature of the source region (Herzberg, 1992).

The oldest komatiitic volcanism was presumably started by the first slabs subducting below the shell and displacing it to shallower depths. The volatile-bearing plumes formed by partial melting of these slabs underwent substantial heating by passing through the overlying segments of the shell. Extensive melting, generating komatiitic melts, occurred at the intersection of the adiabat corresponding to the P–T trajectories of these rising overheated plumes and the anhydrous mantle solidus.

Fig. 10 shows schematically the thermal structure of the upper mantle containing a shell segment displaced to shallower depths by the underlying slab. Modified KLB-1 solidus (Gasparik, 1992) is an approximation of the mantle solidus. Takahashi (1990) estimated the maximum potential mantle temperature (adiabat at zero pressure) of the corresponding Archean mantle at 1750°C from the origin of the oldest komatiites. The resulting origin at 300 km depth and at a temperature in excess of 1900°C is similar to the conditions reported by Herzberg (1992).

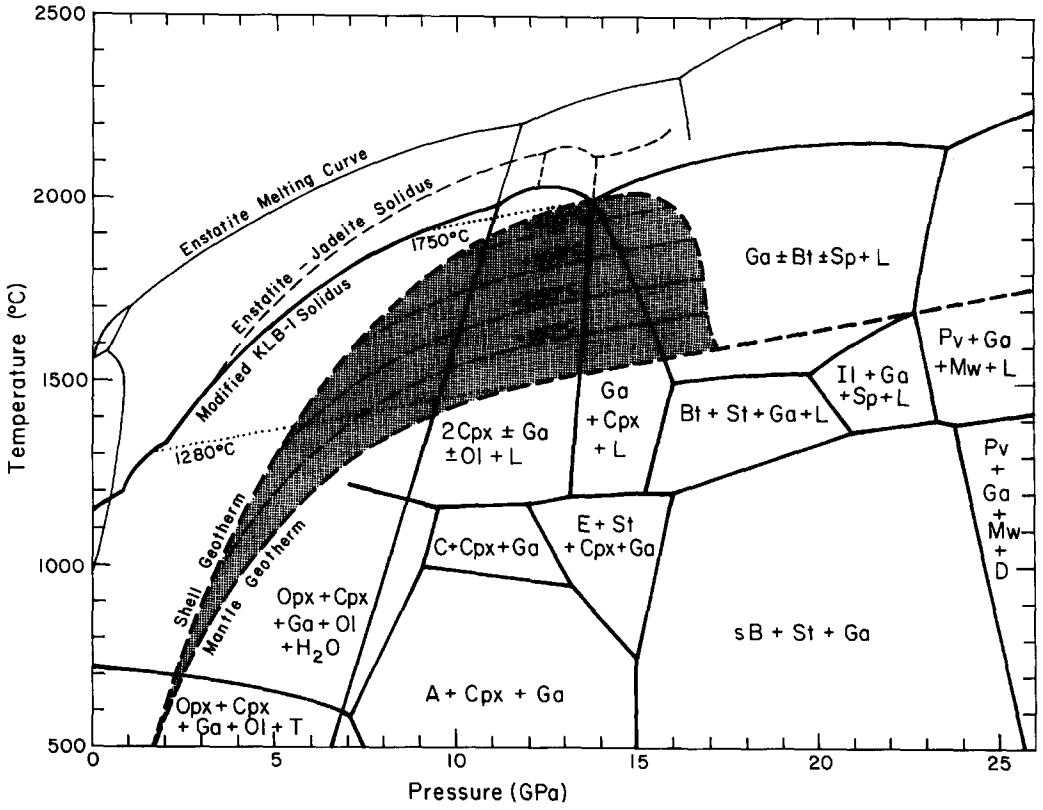

Fig. 10. Temperature–pressure phase diagram for a volatile-bearing mantle. Dash–dot isotherms indicate shell temperatures in excess of the normal mantle temperatures corresponding to the mantle geotherm based on the potential mantle temperature of 1280°C. Shell geotherm is based on the potential mantle temperature for the Archean of 1750°C (Takahashi, 1990). A, Phase A; C, phase C (could also include clinohumite or chondrodite); D, phase D; E, phase E; sB, superhydrous phase B; T, talc; other symbols as in Fig. 1, Fig. 4 and Fig. 5. Phase relations are based on Presnall and Gasparik (1990), Gasparik (1992, 1993) and Zhang and Herzberg (1994).

This can be compared with the potential temperature of the basalt-generating mantle at 1280°C (McKenzie and Bickle, 1988), which has remained fairly constant during the Earth's history.

9. Conclusion

The model for the Earth's upper mantle shown in Fig. 7 is similar to that proposed by Gasparik (1993). The main contribution of the present study is the verification that such a layered upper mantle can have an average composition corresponding to the cosmic abundances of elements. At the same time, its structure is consistent with the experimentally determined phase relations, and appears to have sufficient flexibility to match the observed seismic velocity profiles. The proposed structure can be produced by accumulation of olivine-rich crust in the upper 200 km of the magma ocean, and does not require garnet fractionation, which seems inconsistent with the geochemical evidence.

The implications of a hidden reservoir in the upper mantle for our understanding of mantle chemistry are far reaching. The potential existence of such a reservoir could provide an explanation for the discrepancy between the chemistry of the observable portion of the upper mantle and the cosmic abundances of elements, including depletions in many trace elements. If the sodium content of the upper mantle corresponds to its cosmic abundance, it is likely that neither potassium is depleted, and its high concentration in the shell could be a major source of radiogenic heating. The radiogenic heating could also play a more important role in the lower mantle than is generally assumed.

Acknowledgements

This study was funded by National Science Foundation Grant EAR 93-03865.

References

Abe, Y., 1993. Thermal evolution and chemical differentiation of the terrestrial magma ocean. Geophys. Monogr. (IUGG 14), 74: 41–54.

Agee, C.B. and Li, J., 1996. Pressure effect on partitioning of nickel, cobalt, and sulfur during mantle–core formation. J. Conf. Abstr., 1(1): 510.

Agee, C.B. and Walker, D., 1988. Mass balance and phase density constraints on early differentiation of chondritic mantle. Earth Planet. Sci. Lett., 90: 144–156.

Agee, C.B. and Walker, D., 1993. Olivine flotation in mantle melt. Earth Planet. Sci. Lett., 114: 315–324.

Allègre, C.J., 1995. Geochemical structure and evolution of the mantle. EOS Trans. Am. Geophys. Union, Spring Meet. Suppl., 76(17): S294.

Anders, E. and Grevesse, N., 1989. Abundances of the elements: meteoritic and solar. Geochim. Cosmochim. Acta, 53: 197–214.

Anderson, D.L., 1979. Chemical stratification of the mantle. J. Geophys. Res., 84: 6297–6298.

Anderson, D.L., 1982. Isotopic evolution of the mantle: a model. Earth Planet. Sci. Lett., 57: 13–24.

Anderson, D.L., 1989. Theory of the Earth. Blackwell Scientific, Oxford.

Anderson, D.L., Tanimoto, T. and Zhang, Y., 1992. Plate tectonics and hotspots: the third dimension. Science, 256: 1645–1651.

Arndt, N.T., 1986. Komatiites: a dirty window to the Archean mantle. Terra Cognita, 6: 59–66.

Bass, J.D. and Anderson, D.L., 1984. Composition of the upper mantle: geophysical tests of two petrological models. Geophys. Res. Lett., 11: 229–232.

Basu, A.R., Ray, S.L., Saha, A.K. and Sarkar, S.N., 1981. Eastern Indian 3800-million-year-old crust and early mantle differentiation. Science, 212: 1502–1506.

Benz, H.M. and Vidale, J.E., 1993. Sharpness of upper-mantle discontinuities determined from high-frequency reflections. Nature, 365: 147–150.

Bickle, M.J., Ford, C.E. and Nisbet, E.G., 1977. The petrogenesis of peridotitic komatiites: evidence from high-pressure melting experiments. Earth Planet. Sci. Lett., 37: 97–106.

Cameron, A.G.W. and Benz, W., 1991. The origin of the moon and the single impact hypothesis. Icarus, 92: 204–216.

Cameron, A.G.W. and Ward, W.R., 1976. The origin of the moon. Lunar Sci., 7: 120–122.

Dicke, R.H., 1969. Average acceleration of the Earth's rotation and the viscosity of the deep mantle. J. Geophys. Res., 74: 5895–5902.

Drake, M.J., McFarlane, E.A., Gasparik, T. and Rubie, D.C., 1993. Mg-perovskite/silicate melt and majorite garnet/silicate melt partition coefficients in the system $CaO–MgO–SiO_2$ at high temperatures and pressures. J. Geophys. Res., 98: 5427–5431.

Forte, A.M., Peltier, W.R. and Dziewonski, A.M., 1991. Inferences of mantle viscosity from tectonic plate velocities. Geophys. Res. Lett., 18: 1747–1750.

Fukao, Y., Obayashi, M., Inoue, H. and Nenbai, M., 1992. Subducting slabs stagnant in the mantle transition zone. J. Geophys. Res., 97: 4809–4822.

Galer, S.J.G. and Goldstein, S.L., 1991. Early mantle differentia-

tion and its thermal consequences. Geochim. Cosmochim. Acta, 55: 227–239.

Gasparik, T., 1989. Transformation of enstatite–diopside–jadeite pyroxenes to garnet. Contrib. Mineral. Petrol., 102: 389–405.

Gasparik, T., 1990a. Immiscibility in the majorite garnets. EOS Trans. Am. Geophys. Union, 71: 1587.

Gasparik, T., 1990b. Phase relations in the transition zone. J. Geophys. Res., 95: 15751–15769.

Gasparik, T., 1992. Enstatite–jadeite join and its role in the Earth's mantle. Contrib. Mineral. Petrol., 111: 283–298.

Gasparik, T., 1993. The role of volatiles in the transition zone. J. Geophys. Res., 98: 4287–4299.

Gasparik, T., 1996a. Melting experiments on the enstatite–diopside join at 70–224 kbar, including the melting of diopside. Contrib. Mineral. Petrol., 124: 139–153.

Gasparik, T., 1996b. Diopside-jadeite join at 16–22 GPa. Phys. Chem. Minerals, 23: 476–486.

Gasparik, T. and Drake, M.J., 1995. Partitioning of elements among two silicate perovskites, superphase B, and volatile-bearing melt at 23 GPa and 1500–1600°C. Earth Planet. Sci. Lett., 134: 307–318.

Hamilton, P.J., O'Nions, R.K., Bridgwater, D. and Nutman, A., 1983. Sm–Nd studies of Archaean metasediments and metavolcanics from West Greenland and their implications for the Earth's early history. Earth Planet. Sci. Lett., 62: 263–272.

Hart, S.R., 1988. Heterogeneous mantle domains: signatures, genesis and mixing chronologies. Earth Planet. Sci. Lett., 90: 273–296.

Hartmann, W.K. and Davis, D.R., 1975. Satellite-sized planetesimals and lunar origin. Icarus, 24: 504–515.

Herzberg, C., 1992. Depth and degree of melting of komatiites. J. Geophys. Res., 97: 4521–4540.

Herzberg, C. and Gasparik, T., 1991. Garnet and pyroxenes in the mantle: a test of the majorite fractionation hypothesis. J. Geophys. Res., 96: 16263–16274.

Herzberg, C., Gasparik, T. and Sawamoto, H., 1990. Origin of mantle peridotite: constraints from melting experiments to 16.5 GPa. J. Geophys. Res., 95: 15779–15803.

Jagoutz, E., Palme, H., Baddenhausen, H., Blum, K., Cendales, M., Dreibus, G., Spettel, B., Lorenz, V. and Wanke, H., 1979. The abundances of major, minor, and trace elements in the earth's mantle as derived from primitive ultramafic nodules. Proc. 10th Lunar Planet. Sci. Conf., pp. 2031–2050.

Jordan, T.H., 1975. The continental tectosphere. Rev. Geophys. Space Phys., 13(3): 1–12.

Karato, S., Wang, Z., Liu, B. and Fujino, K., 1995. Plastic deformation of garnets: systematics and implications for the rheology of the mantle transition zone. Earth Planet. Sci. Lett., 130: 13–30.

Kato, T., Ringwood, A.E. and Irifune, T., 1988a. Experimental determination of element partitioning between silicate perovskites, garnets and liquids: constraints on early differentiation of the mantle. Earth Planet. Sci. Lett., 89: 123–145.

Kato, T., Ringwood, A.E. and Irifune, T., 1988b. Constraints on element partition coefficients between $MgSiO_3$ perovskite and liquid determined by direct measurements. Earth Planet. Sci. Lett., 90: 65–68.

Katsura, T. and Ito, E., 1989. The system Mg_2SiO_4–Fe_2SiO_4 at high pressures and temperatures: precise determination of stabilities of olivine, modified spinel, and spinel. J. Geophys. Res., 94: 15663–15670.

King, S.D. and Masters, G., 1992. An inversion for radial viscosity structure using seismic tomography. Geophys. Res. Lett., 19: 1551–1554.

Knopoff, L., 1964. The convection current hypothesis. Rev. Geophys., 2: 89–122.

Kumazawa, M., 1981. Origin of materials in the Earth's interior and their layered distribution. Jpn. J. Petrol. Mineral. Econ. Geol., Spec. Issue, 3: 239–247.

Liu, L., 1979. On the 650-km seismic discontinuity. Earth Planet. Sci. Lett., 42: 202–208.

Liu, M., 1994. Asymmetric phase effects and mantle convection patterns. Science, 264: 1904–1907.

MacDonald, G.J.F., 1963. The deep structure of continents. Rev. Geophys., 1: 587–665.

MacDonald, G.J.F. and Knopoff, L., 1958. On the chemical composition of the outer core. Geophys. J. R. Astron. Soc., 1: 284–297.

McCulloch, M.T., 1993. The role of subducted slabs in an evolving earth. Earth Planet. Sci. Lett., 115: 89–100.

McCulloch, M.T. and Compston, W., 1981. Sm–Nd age of Kambalda and Kanowna greenstones and heterogeneity in the Archean mantle. Nature, 294: 322–327.

McKenzie, D. and Bickle, M.J., 1988. The volume and composition of melt generated by extension of the lithosphere. J. Petrol., 29: 625–679.

Miller, G.H., Stolper, E.M. and Ahrens, T.J., 1991. The equation of state of molten komatiite: 1. Shock wave compression to 36 GPa, 2. Application to komatiite petrogenesis and the Hadean mantle. J. Geophys. Res., 96: 11831–11864.

Morse, S.A., 1993. Behavior of a perched crystal layer in a magma ocean. J. Geophys. Res., 98: 5347–5353.

Nolet, G., Grand, S.P. and Kennett, B.L.N., 1994. Seismic heterogeneity in the upper mantle. J. Geophys. Res., 99: 23753–23766.

O'Nions, R.K. and Tolstikhin, I.N., 1996. Limits on the mass flux between lower and upper mantle and stability of layering. Earth Planet. Sci. Lett., 139: 213–222.

Ohtani, E., 1985. The primordial terrestrial magma ocean and its implications for stratification of the mantle. Earth Planet. Sci. Lett., 38: 70–80.

Ohtani, E., Kawabe, I., Moriyama, J. and Nagata, Y., 1989. Partitioning of elements between majorite garnet and melt and implications for petrogenesis of komatiite. Contrib. Mineral. Petrol., 103: 263–269.

Ohtani, E., Kagawa, N. and Fujino, K., 1991. Stability of majorite $(Mg,Fe)SiO_3$ at high pressures and 1800°C. Earth Planet. Sci. Lett., 102: 158–166.

Ohtani, E., Suzuki, A. and Kato, T., 1993. Flotation of olivine in the peridotite melt at high pressure. Proc. Jpn. Acad., 69(B): 23–28.

Ohtani, E., Nagata, Y., Suzuki, A. and Kato, T., 1995. Melting relations of peridotite and the density crossover in planetary mantles. Chem. Geol., 120: 207–221.

Palme, H. and Nickel, K.G., 1985. Ca/Al ratio and the composition of the Earth's mantle. Geochim. Cosmochim. Acta, 49: 2123–2132.

Pollack, H.N. and Chapman, D.S., 1977. On the regional variation of heat flow, geotherms and lithospheric thickness. Tectonophysics, 38: 279–296.

Presnall, D.C. and Gasparik, T., 1990. Melting of enstatite ($MgSiO_3$) from 10 to 16.5 GPa and the forsterite (Mg_2SiO_4)–majorite ($MgSiO_3$) eutectic at 16.5 GPa: implications for the origin of the mantle. J. Geophys. Res., 95: 15771–15777.

Presnall, D.C. and Walter, M.J., 1993. Melting of forsterite, Mg_2SiO_4, from 9.7 to 16.5 GPa. J. Geophys. Res., 98: 19777–19783.

Rapp, R.P. and Shimizu, N., 1996. Arc magmatism in hot subduction zones: interactions between slab-derived melts and the mantle wedge, and the petrogenesis of adakites and high-magnesian andesites (HMA). J. Conf. Abstr., 1(1): 497.

Revenaugh, J. and Sipkin, S.A., 1994. Seismic evidence for silicate melt atop the 410-km mantle discontinuity. Nature, 369: 474–476.

Ricard, Y., Vigny, C. and Froidevaux, C., 1989. Mantle heterogeneities, geoid and plate motion: a Monte Carlo inversion. J. Geophys. Res., 94: 13739–13754.

Rigden, S.M., Ahrens, T.J. and Stolper, E.M., 1984. Densities of liquid silicates at high pressures. Science, 226: 1071–1074.

Rigden, S.M., Gwanmesia, G.D. and Liebermann, R.C., 1994. Elastic wave velocities of a pyrope–majorite garnet to 3 GPa. Phys. Earth Planet. Inter., 86: 35–44.

Righter, K., Drake, M.J. and Yaxley, G., 1996. Predicting siderophile element metal–silicate partition coefficients. J. Conf. Abstr., 1(1): 510.

Ringwood, A.E., 1962. A model for the upper mantle. J. Geophys. Res., 67: 857–867.

Ringwood, A.E., 1994. Role of the transition zone and 660 km discontinuity in mantle dynamics. Phys. Earth Planet. Inter., 86: 5–24.

Ringwood, A.E. and Irifune, T., 1988. Nature of the 650-km seismic discontinuity: implications for mantle dynamics and differentiation. Nature, 331: 131–136.

Shirey, S. and Hanson, G.N., 1986. Mantle heterogeneity and crustal recycling in Archean granite–greenstone belts: evidence from Nd isotopes and trace elements in the Rainy Lakes area, Superior Province, Ontario, Canada. Geochim. Cosmochim. Acta, 50: 2631–2651.

Silver, P.G., Beck, S.L., Wallace, T.C., Meade, C., Myers, S.C., James, D.E. and Kuehnel, R., 1995. Rupture characteristics of the deep Bolivian earthquake of 9 June 1994 and the mechanism of deep-focus earthquakes. Science, 268: 69–73.

Solomatov, V.S. and Stevenson, D.J., 1993. Nonfractional crystallization of a terrestrial magma ocean. J. Geophys. Res., 98: 5391–5406.

Stevenson, D.J., 1987. Origin of the moon—the collision hypothesis. Annu. Rev. Earth Planet. Sci., 15: 271–315.

Stolper, E.M., Walker, D., Hager, B.H. and Hays, J.F., 1981. Melt segregation from partially molten source region: the importance of melt density and source region size. J. Geophys. Res., 86: 6161–6271.

Sweeney, J.S. and Heinz, D.L., 1995. Irreversible melting of magnesium–iron–silicate perovskite at lower mantle pressures. EOS Trans. Am. Geophys. Union, Fall Meet. Suppl., 76(46): F553.

Takahashi, E., 1990. Speculations on the Archean mantle: missing link between komatiite and depleted garnet peridotite. J. Geophys. Res., 95: 15941–15954.

Tonks, W.B. and Melosh, H.J., 1990. The physics of crystal settling and suspension in a turbulent magma ocean. In: N.E. Newsom and J.H. Jones (Editors), Origin of the Earth. Oxford University Press, New York, pp. 151–174.

Tonks, W.B. and Melosh, H.J., 1993. Magma ocean formation due to giant impacts. J. Geophys. Res., 98: 5319–5333.

Van den Berg, A.P., van Keken, P.E. and Yuen, D.A., 1993. High melting temperature of perovskite: dynamic implications for creep in the lower mantle. EOS Trans. Am. Geophys. Union, Fall Meet. Suppl., 74(43): 557.

Van der Hilst, R., Engdahl, R., Spakman, W. and Nolet, G., 1991. Tomographic imaging of subducted lithosphere below northwest Pacific island arcs. Nature, 353: 37–43.

Wei, K., Trønnes, R.G. and Scarfe, C.M., 1990. Phase relations of aluminum-undepleted and aluminum-depleted komatiites at pressures of 4–12 GPa. J. Geophys. Res., 95: 15817–15827.

Weinstein, S.A., 1992. Induced compositional layering in a convecting fluid layer by an endothermic phase transition. Earth Planet. Sci. Lett., 113: 23–39.

Wetherill, G.W., 1976. The role of large bodies in the formation of the solar system. Proc. 7th Lunar Planet. Sci. Conf., pp. 3245–3257.

Zerr, A. and Boehler, R., 1993. Melting of $(Mg,Fe)SiO_3$-perovskite to 625 kilobars: indications of a high melting temperature in the lower mantle. Nature, 262: 553–555.

Zhang, J. and Herzberg, C., 1994. Melting experiments on anhydrous peridotite KLB-1 from 5.0 to 22.5 GPa. J. Geophys. Res., 99: 17729–17742.

Zielhuis, A. and Nolet, G., 1994. Deep seismic expression of an ancient plate boundary in Europe. Science, 265: 79–81.